



## Research article



# Is aryl hydrocarbon receptor antagonism after ischemia effective in alleviating acute hepatic ischemia-reperfusion injury in rats?

Jae-Im Kwon<sup>a</sup>, Hwon Heo<sup>b</sup>, Yeon Ji Chae<sup>b</sup>, Joongkee Min<sup>b</sup>, Do-Wan Lee<sup>b</sup>, Sang Tae Kim<sup>c</sup>, Monica Young Choi<sup>b</sup>, Yu Sub Sung<sup>d</sup>, Kyung Won Kim<sup>e</sup>, Yoonseok Choi<sup>f</sup>, Dong Cheol Woo<sup>a,c,\*\*</sup>, Chul-Woong Woo<sup>c,\*</sup>

<sup>a</sup> Department of Medical Science, AMIST, Asan Medical Center, University of Ulsan College of Medicine, Seoul, Republic of Korea

<sup>b</sup> Asan Institute for Life Sciences, Asan Medical Center, 88, Olympic-ro 43-gil, Songpa-gu, Seoul, Republic of Korea

<sup>c</sup> Convergence Medicine Research Center, Asan Medical Center, 88, Olympic-ro 43-gil, Songpa-gu, Seoul, Republic of Korea

<sup>d</sup> Clinical Research Center, Asan Medical Center, 88, Olympic-ro 43-gil, Songpa-gu, Seoul, Republic of Korea

<sup>e</sup> Department of Radiology, Asan Medical Center, 88, Olympic-ro 43-gil, Songpa-gu, Seoul, Republic of Korea

<sup>f</sup> Medical Research Institute, Gangneung Asan Hospital, 38, Bangdong-gil, Sacheon-myeon, Gangneung-si, Gangwon-do, Republic of Korea

## ARTICLE INFO

## Keywords:

Liver  
Ischemia  
Reperfusion  
Aryl hydrocarbon receptor  
Magnetic resonance imaging  
L-kynurenine

## ABSTRACT

Aryl hydrocarbon receptors (AhRs) have been reported to be important mediators of ischemic injury in the brain. Furthermore, the pharmacological inhibition of AhR activation after ischemia has been shown to attenuate cerebral ischemia-reperfusion (IR) injury. Here, we investigated whether AhR antagonist administration after ischemia was also effective in ameliorating hepatic IR injury. A 70% partial hepatic IR (45-min ischemia and 24-h reperfusion) injury was induced in rats. We administered 6,2',4'-trimethoxyflavone (TMF, 5 mg/kg) intraperitoneally 10 min after ischemia. Hepatic IR injury was observed using serum, magnetic resonance imaging-based liver function indices, and liver samples. TMF-treated rats showed significantly lower relative enhancement (RE) values and serum alanine aminotransferase (ALT) and aspartate aminotransferase levels than did untreated rats at 3 h after reperfusion. After 24 h of reperfusion, TMF-treated rats had significantly lower RE values,  $\Delta T1$  values, serum ALT levels, and necrotic area percentage than did untreated rats. The expression of the apoptosis-related proteins, Bax and cleaved caspase-3, was significantly lower in TMF-treated rats than in untreated rats. This study demonstrated that inhibition of AhR activation after ischemia was effective in ameliorating IR-induced liver injury in rats.

## 1. Introduction

Hepatic ischemia-reperfusion (IR) injury commonly occurs during liver transplantation or resection and is considered a leading cause of liver damage and dysfunction [1–5]. The mechanisms of hepatic IR injury have been extensively investigated, but nevertheless remain largely unclear. Furthermore, although anaerobic metabolism, mitochondria, oxidative stress, intracellular calcium overload, liver Kupffer cells, neutrophils, cytokines, and chemokines have been found to be involved in the hepatic IR injury process, effective

\* Corresponding author

\*\* Corresponding author

E-mail addresses: [dcwoo@amc.seoul.kr](mailto:dcwoo@amc.seoul.kr) (D.C. Woo), [wandj79@hanmail.net](mailto:wandj79@hanmail.net) (C.-W. Woo).

<https://doi.org/10.1016/j.heliyon.2023.e15596>

Received 20 April 2022; Received in revised form 11 April 2023; Accepted 14 April 2023

Available online 28 April 2023

2405-8440/© 2023 The Authors. Published by Elsevier Ltd. This is an open access article under the CC BY-NC-ND license (<http://creativecommons.org/licenses/by-nc-nd/4.0/>).

prevention or treatment in clinical practice is still lacking [6].

The aryl hydrocarbon receptor (AhR) is a ligand-activated basic helix-loop-helix/Per-ARNT-Sim transcription factor known to mediate toxic and carcinogenic effects of xenobiotics [7,8]. Upon ligand bindings, AhR translocates to the nucleus to form an active heterodimeric complex and induces rapid transcriptional activations in various organs and cellular systems [9]. Recent studies have suggested that cerebral ischemia induces AhR activation and exacerbates neuronal damage [10,11]. This is because L-kynurenine (L-Kyn), an endogenous ligand of AhR, is accumulated in the brain during ischemia and triggers the activation of AhR [10]. Moreover, the pharmacological manipulation of AhR activation after ischemia has been shown to modulate neuronal damage due to cerebral IR *in vivo* [12]. Observations in the brain raise the possibility that similar pathways can be involved in the liver. Because L-Kyn is produced in a significant amount in the liver through the degradation of L-tryptophan by tryptophan-2,3-dioxygenase (TDO) [13], it is more likely to accumulate in the liver than in the brain due to ischemia. This means that ischemia-induced AhR activation and tissue damage after reperfusion could be greater in the liver than in the brain. Therefore, the inhibition of AhR activation after ischemia is considered to be effective in suppressing hepatic IR injury. However, to the best of our knowledge, the effects of AhR antagonism on hepatic IR injury have not yet been reported.

In the present study, we investigated the protective effects of AhR antagonism after ischemia in a rat hepatic IR injury model. Moreover, we used *in vivo* magnetic resonance imaging (MRI) and molecular biological techniques to evaluate whether the administration of an AhR antagonist influences the hepatoprotective effects of AhR antagonism.

## 2. Materials and methods

### 2.1. Ethics statements

The present study was performed following approval by the Institutional Animal Care and Use Committee of Asan Medical Center (IACUC Number: 2019-02-035), and all included procedures were performed in strict accordance with the guidelines of the Association for Assessment and Accreditation of Laboratory Animal Care. All involved experiments are reported in accordance with the ARRIVE guidelines (Animal Research: Reporting in Vivo Experiments) for how to REPORT animal experiments. All animal surgeries were performed under isoflurane anesthesia and were closely monitored by trained individuals capable of assessing the animals' pain-related behaviors. Euthanasia was planned if the animals exhibited persistent pain-related behaviors, although no animals exhibited severe pain-related behaviors during the experimental period.

### 2.2. 70% partial hepatic IR injury model

Sprague-Dawley rats (male; 8 weeks old; weight, 290–310 g; Orient Bio, Pyeongtaek, Republic of Korea) were used in the experiments. All the rats were housed, three per cage, in a 12-h light-dark cycle with consistent temperature at 24–25 °C and unrestricted access to food and water.

Based on previous studies, a 70% partial hepatic IR injury model was established in rats [4,14]. Briefly, the abdominal cavity was exposed by a midline incision, and the portal triad (hepatic artery, portal vein, and bile duct), which supplied the left lateral and median lobes, was clamped with an atraumatic, microvascular clamp (Fig. 1). The clamp was removed 45 min after ischemia developed, and the abdomen was closed in a single layer. Successful induction of 70% partial ischemia of the liver was visually confirmed by the blanching of ischemic lobes compared to non-ischemic lobes (right and caudate lobes). Successful reperfusion was also determined by the color of ischemic lobes turning back to that of the non-ischemic lobes. All rats were initially anesthetized using 5% isoflurane in 70% N<sub>2</sub>O/30% O<sub>2</sub> (flow rate, 1.0 L/min), and anesthesia was maintained using 2% isoflurane during surgery. Rats with no visual changes in the left and median lobes by IR induction were excluded.

### 2.3. Drug treatment

As the AhR antagonist, 5 mg/kg of 6,2',4'-trimethoxyflavone (TMF, Sigma-Aldrich, St. Louis, MO, USA) dissolved in 2% dimethyl sulfoxide (DMSO, Sigma-Aldrich) was used [15]. An equal volume of DMSO was used for the vehicle-treated control group. All treatments were administered via intraperitoneal injection.

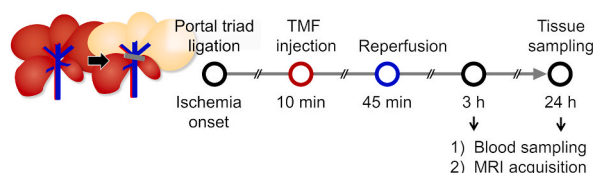


**Fig. 1. Schematic diagram of the experimental procedure** Hepatic ischemia was induced by clamping the portal triad for 45 min followed by reperfusion. Afterwards, 6,2',4'-trimethoxyflavone was administered 10 min after ischemia. Blood samples and magnetic resonance imaging data were obtained at 3 and 24 h after reperfusion. Liver tissues were harvested at 24 h after reperfusion.

## 2.4. Animal groups

The rats were randomly divided into the following: (1) a sham group without no IR modeling and with vehicle injection (n = 8); (2) a control group with IR modeling and vehicle injection (n = 8); and (3) a TMF group with IR modeling and administration of the drug at 10 min after ischemia (n = 8).

## 2.5. MRI analysis

MRI was performed on a 9.4 T MRI system (Agilent Technologies, Santa Clara, CA, USA) with a 63-mm transmit/receive volume coil. The animals were maintained under respiratory anesthesia with 2.0–2.5% isoflurane in a 1:2 mixture of O<sub>2</sub>:N<sub>2</sub>O and body temperature of 37.5 ± 0.5 °C through an air heater system during image acquisition. These were continuously monitored for stable breathing.

MRI data were obtained at 3 and 24 h after reperfusion. The MRI protocols included T1-weighted gradient echo images (T1-WI) and T1 mapping. The parameters for each sequence are shown in [Supplementary Table S1](#). MRI images were obtained before and 20 min after administration of Gd-EOB-DTPA (25 μM/kg, Primovist, Bayer Korea, South Korea) [16].

All MRI data were analyzed using the ImageJ software (National Institutes of Health, Bethesda, MA, USA; <https://rsbweb.nih.gov/ij/>) by an observer blind to grouping information. The mean SI values and T1 relaxation time were measured on T1-WIs and T1 maps obtained before and 20 min after Gd-EOB-DTPA administration. Region of interests (ROIs) were manually placed at identical locations on the hepatic parenchyma and paravertebral muscle in T1-WIs and T1 maps. The ROIs on hepatic parenchyma were placed by avoiding visible blood vessels or imaging artifacts. Two ROIs were randomly placed in the liver and paravertebral muscles in the T1-WIs and T1 maps before and after Gd-EOB-DTPA administration (Fig. 2). The mean signal intensity (SI) and T1 values for both ROIs in the liver were considered representative SI and T1 values of the whole liver, respectively. The mean SI values for both ROIs in the paravertebral muscle were regarded as the representative SI values for the entire paravertebral muscle. The size of the ROIs ranged from 10 to 11 mm<sup>2</sup> in liver parenchyma and 8–9 mm<sup>2</sup> in paravertebral muscles. MRI-based liver function indices were calculated from the SI measurements or T1 relaxation time before (SI<sub>pre</sub>, T1<sub>pre</sub>) and 20 min after (SI<sub>post</sub>, T1<sub>post</sub>) Gd-EOB-DTPA administration as follows: (1) relative enhancement (RE) of the liver = (SI<sub>post</sub> – SI<sub>pre</sub>)/SI<sub>pre</sub>; (2) liver-to-muscle ratio (LMR) = SI<sub>post</sub> of the liver/SI<sub>post</sub> of the muscle; (3) T1<sub>post</sub> = T1<sub>post</sub> values of the liver; and (4) ΔT1 = T1<sub>pre</sub> – T1<sub>post</sub> [17,18].

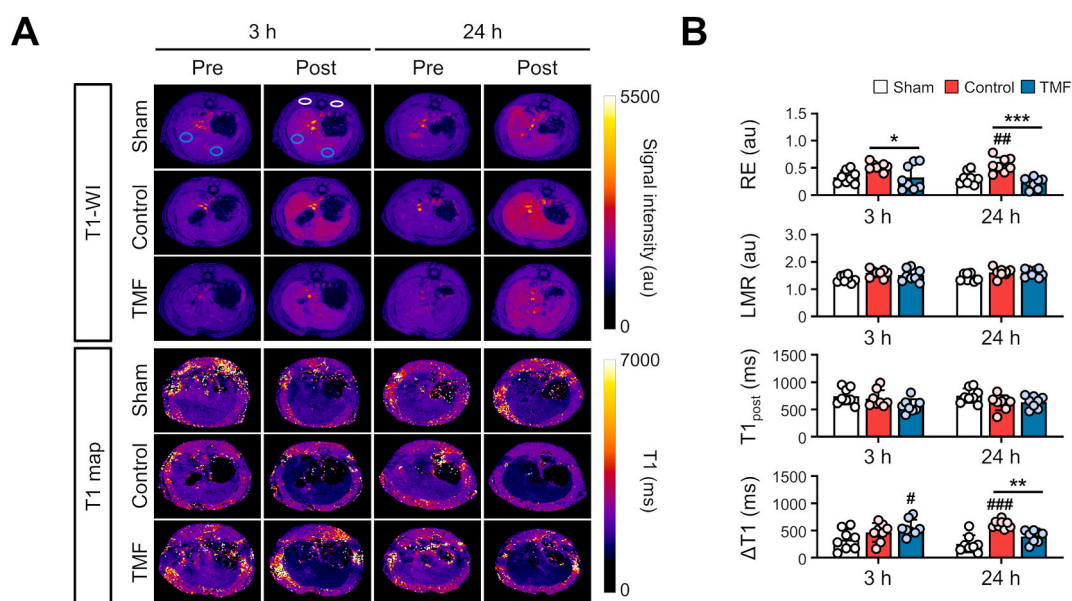


**Fig. 2.** Effect of 6,2',4'-trimethoxyflavone (TMF) treatment on magnetic resonance imaging-based liver function indices (A) Representative T1-weighted gradient echo images and T1 maps at 3 and 24 h after reperfusion. Mean signal intensity (SI) and T1 values were measured in the liver (blue circles). Mean SI values were measured in the paravertebral muscle (white circles). (B) The relative enhancement (RE) values at 24 h after reperfusion were significantly higher in the control group than in the sham group. At 3 and 24 h after reperfusion, the RE values were significantly decreased in the TMF group than in the control group. The ΔT1 values at 3 h after reperfusion were significantly higher in the TMF group than in the sham group. The ΔT1 values at 24 h after reperfusion were significantly higher in the control group than in the sham group. At 24 h after reperfusion, the ΔT1 values were significantly decreased in the TMF group than in the control group. Data are represented as means ± standard deviations (n = eight rats in each group). #P < 0.05 vs. sham group; ##P < 0.01 vs. sham group; ###P < 0.001 vs. sham group; \*P < 0.05 vs. control group; \*\*P < 0.01 vs. control group; \*\*\*P < 0.001 vs. control group. (For interpretation of the references to color in this figure legend, the reader is referred to the Web version of this article.)

## 2.6. Measurement of serum enzymes

Blood samples were obtained from the rats' jugular veins 3 and 24 h after reperfusion. The samples were centrifuged at 2000 r/minutes for 14 min to obtain serum for analysis. The activities of serum alanine aminotransferase (ALT) and aspartate aminotransferase (AST) were determined with a biochemical analyzer (7180, Hitachi, Tokyo, Japan).

## 2.7. Hematoxylin and eosin (H&E) staining

Liver tissues were harvested at 24 h after reperfusion and fixed in 4% paraformaldehyde (Biosesang, Seongnam, Republic of Korea). Fixed tissues were embedded in paraffin, and the tissues were sectioned to 3- $\mu$ m thickness. H&E staining was performed using an automatic stainer (Leica, Wetzlar, Germany). The percentages of necrotic areas in five random sections per slide were analyzed under a microscope at a magnification of  $\times 50$  (Vectra, PerkinElmer, MA, USA) [19].

## 2.8. Terminal deoxynucleotidyl transferase-mediated dUTP nick-end labeling (TUNEL) assay

A TUNEL assay was performed to detect apoptotic cells using a commercially available apoptosis detection kit (Millipore, Billerica, MA, USA) according to the manufacturer's instructions. Paraffin-embedded liver tissue sections were treated with a mixture of reaction buffer and enzyme (7:3) at 37 °C for 1 h, and the *anti*-digoxigenin peroxidase conjugate was treated at room temperature for 30 min. Thereafter, the tissue was treated with DAB substrate (3,3' diaminobenzidine tetrahydrochloride hydrate, Sigma-Aldrich) (1:50) in the dark for 5 min, and then stained with hematoxylin (Sigma-Aldrich) for 2 min in the dark. TUNEL-positive cells were observed under a microscope at a magnification of  $\times 200$  (Vectra, PerkinElmer, MA, USA).

## 2.9. Western blot

Liver tissues from the sham (5 mg), control (30 mg), and TMF groups (30 mg) were centrifuged in cold-PBS at 500 $\times$ g and at 4 °C for 5 min and homogenized in radio-immunoprecipitation buffer (Sigma-Aldrich, MO, USA) with 1  $\times$  protease inhibitor cocktail (Sigma-Aldrich) on ice. After 30 min, the lysate was centrifuged at 13,000 rpm and at 4 °C for 20 min. The supernatant was aliquoted into a 1.5-mL tube and quantified using a bicinchoninic acid assay (ThermoFisher Scientific, MA, USA). In total, 30- $\mu$ g protein was separated in 8% pre-made sodium dodecyl sulfate-polyacrylamide gel electrophoresis (ThermoFisher Scientific) and transferred to a polyvinylidene fluoride membrane (ThermoFisher Scientific). The membrane was blocked with 5% skim milk (Becton and Dickinson [BD], NJ, USA) in 1  $\times$  tris-buffered saline (Elpis-Biotech, Daejeon, Republic of Korea) with 20 (Sigma-Aldrich) at room temperature for 1 h and then incubated with mouse *anti*-AhR (1:1000, Santa Cruz Biotechnology, TX, USA), rabbit *anti*-Bcl-2 (1:1000, Novus Biologicals, CO, USA), rabbit *anti*-Bax (1:1000, Cell Signaling Technology, MA, USA), rabbit *anti*-cleaved caspase-3 (C-cas3, 1:1000, Cell Signaling Technology), and mouse *anti*-GAPDH (1:10000, ThermoFisher Scientific) at 4 °C overnight. The antibodies were washed three times for 10 min in 1  $\times$  tris-buffered saline, and the membrane was incubated with goat anti-mouse (1:5000, ThermoFisher Scientific) or rabbit (1:2000, ThermoFisher Scientific) immunoglobulin G secondary antibody-horseradish peroxidase conjugate at room temperature for 1 h. The membrane reacted with Lumi Femto Solution A:B (A:B = 1:1, DoGenBio, Seoul, Republic of Korea) of a chemi-luminescence reagent after washing, and AhR was quantified using GAPDH via ImageJ software.

## 2.10. Immunohistochemistry staining

Immunohistochemistry staining was conducted as indicated in the Ultra View Universal DAB Detection kit (Ventana Medical Systems, Inc., Oro Valley, AZ, USA). The slides were incubated at 60 °C for 4 min, Ezprep was treated for deparaffinization, and slides were rinsed with a Tris buffer (pH 7.6). After reacting the slides to the antigen retrieval buffer for 1 h at 100 °C, they were treated with rabbit *anti*-AhR (1:1000, Enzo Life Sciences, NY, USA) for 36 min at 37 °C. The rinsed slides were processed using the DISCOVERY Ultra Map anti/Rabbit HRP for 12 min at 37 °C. Ultraview DAB and DAB H<sub>2</sub>O<sub>2</sub> were treated for 8 min at 37 °C, during which AhR-positive cells were stained brown, before Ultra View COPPER was used to treat washed slides for 4 min at 37 °C. After rinsing, the slides were incubated in hematoxylin for 4 min at 37 °C. Finally, the rinsed slides were exposed to BLUING REAGENT for 4 min at 37 °C before they were washed again. AhR-positive cells were observed under a microscope at a magnification of  $\times 200$  (Vectra, PerkinElmer, Waltham, MA, USA).

## 2.11. Quantitative real-time PCR (qRT-PCR)

Total ribonucleic acid (RNA) was extracted from liver tissues using TRIZOL (Invitrogen, MA, USA). Reverse transcription was performed through cDNA synthesis kit (TAKARA Bio, Otsu, JP). qRT-PCR was carried out using SYBR Green PCR Master Mix (Thermo Fisher Scientific) to detect the expressions of AhRR, CYP1a1, CYP1b1, TDO, indoleamine 2,3-dioxygenase 1 (IDO1) and GAPDH with primers (Supplementary Table S2).

## 2.12. Liquid chromatography-tandem mass spectrometry (LC-MS/MS)

L-Kyn and tryptophan standards, internal standard, and derivatization reagents were purchased from Sigma-Aldrich or CDN

isotopes. All solvents including water were purchased from J. T. Baker.

90–100 mg of liver tissues were homogenized using a Tissue-Lyser (Qiagen, Hilden, Germany) with 800  $\mu$ L chloroform/methanol (2/1, v/v), and the homogenate was incubated at 4 °C for 15 min. An internal standard solution containing tryptophan- $d_5$  was added to reach final concentration to 2  $\mu$ M and mixed well. Samples were centrifuged at 14,000 rpm for 15 min. The supernatant was collected and 200  $\mu$ L each of H<sub>2</sub>O and chloroform was added. Samples were mixed vigorously and centrifuged at 4000 rpm for 20 min. Then, aqueous phase was collected and used for chemical derivatization of amino acids using phenylisothiocyanate. After the reaction, the derivatized amino acids were extracted with 5 mM ammonium acetate in methanol, and ready for LC-MS/MS analysis.

L-Kyn and tryptophan were measured with LC-MS/MS equipped with 1290 HPLC (Agilent, Waldbronn, Germany), 5500 mass spectrometry (Sciex, Toronto, Canada), and a reverse phase column (Zorbax Eclipse XDB-C18 100  $\times$  2 mm). 10  $\mu$ L was injected into the LC-MS/MS system and ionized with turbo spray ionization source. 0.2% formic acid in H<sub>2</sub>O and 0.2% formic acid in acetonitrile were used as mobile phase A and B, respectively. The separation gradient was as follows: hold at 0% B for 0.5 min, 0–95% B for 5 min, 95% B for 1 min, and 95 to 0% B for 0.5 min, then hold at 0% B for 2.5 min. LC flow was 500  $\mu$ L/min, and column temperature was kept at 50 °C. Multiple reactions monitoring was used in positive ion mode, and the extracted ion chromatogram corresponding to the specific transition for each amino acid was used for quantitation. Calibration range was generally 1 nM - 100  $\mu$ M with  $R^2 > 0.99$ . Data analysis was performed by using Analyst 1.7 software.

### 2.13. Statistics

Statistical analyses were performed using the IBM SPSS version 21.0 software (IBM Corp., Armonk, NY, USA). Data in multiple groups were compared using a one-way analysis of variance with Tukey's post-hoc test. All the data are expressed as means  $\pm$  standard deviations. Values of  $P < 0.05$  were considered statistically significant.

## 3. Results

### 3.1. Animal modelling

Visual changes in the color of the median and left lobes of the liver were observed in all rats with induced IR, and no rats died during surgery and the follow-up period.

### 3.2. MRI-based liver function indices

The SIs of the liver in T1-WIs obtained at 3 and 24 h after reperfusion were higher in all three groups at 20 min after the administration than those before the administration of Gd-EOB-DTPA (Fig. 2A). Conversely, the T1 values of the liver in T1 maps were lower in all three groups 20 min after the administration than those before the administration of Gd-EOB-DTPA. The RE values at 24 h after reperfusion were significantly higher in the control group than in the sham group ( $P < 0.01$ , Fig. 2B). The RE values at 3 and 24 h after reperfusion were significantly lower in the TMF group than in the control group ( $P < 0.05$  and  $P < 0.001$ , respectively). The  $\Delta T1$

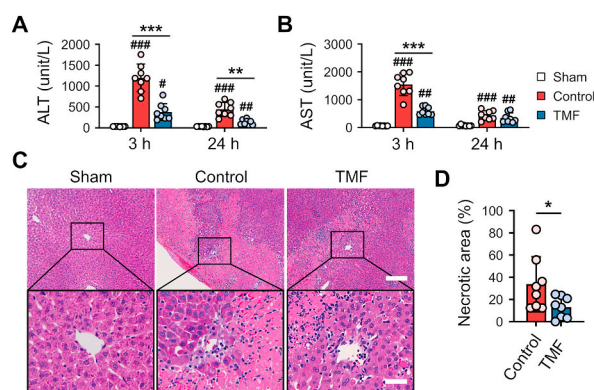


**Fig. 3.** Reduction of serum alanine aminotransferase (ALT) and aspartate aminotransferase (AST) levels and necrotic area by 6,2',4'-trimethoxyflavone (TMF) treatment (A) The control and TMF groups had significantly higher serum ALT levels than did the sham group at 3 and 24 h after reperfusion. Serum ALT levels were significantly lower in the TMF group than in the control group at 3 and 24 h after reperfusion. (B) The control and TMF groups had significantly higher serum AST levels than did the sham group at 3 and 24 h after reperfusion. Serum AST levels were significantly lower in the TMF group than in the control group at 3 h after reperfusion. (C) Representative photomicrographs of hematoxylin and eosin staining 24 h after reperfusion (magnification  $\times$  50, scale bar = 200  $\mu$ m). The upper row shows enlarged versions of the black boxes in the upper row (scale bar = 50  $\mu$ m). (D) The percentage of necrotic area in the TMF group was significantly lower than that in the control group. Data are represented as means  $\pm$  standard deviations ( $n =$  eight rats in each group). \* $P < 0.05$  vs. sham group; \*\* $P < 0.01$  vs. sham group; \*\*\* $P < 0.001$  vs. sham group; \* $P < 0.05$  vs. control group; \*\* $P < 0.01$  vs. control group; \*\*\* $P < 0.001$  vs. control group.

values at 3 h after reperfusion were significantly higher in the TMF group than in the sham group. The  $\Delta T1$  values at 24 h after reperfusion were significantly higher in the control group than in the sham group ( $P < 0.001$ ). The  $\Delta T1$  values at 24 h after reperfusion were significantly lower in the TMF group than in the control group ( $P < 0.01$ ). However, there were no significant differences in the LMR and  $T1_{\text{post}}$  values among the sham, control, and TMF groups ( $P > 0.05$ ).

### 3.3. Changes in serum ALT and AST levels

Compared with the sham group, the control and TMF groups had significantly higher serum ALT and AST levels at 3 and 24 h after reperfusion ( $P < 0.05$ , Fig. 3A and B). The serum ALT levels were significantly lower in the TMF group than in the control group at 3 ( $P < 0.001$ ) and 24 ( $P < 0.01$ ) hours after reperfusion. The serum AST levels were significantly lower in the TMF group than in the control group at 3 h after reperfusion ( $P < 0.001$ ), but no significant difference was observed between the control and TMF groups at 24 h after reperfusion ( $P = 0.422$ ).

### 3.4. Reduction of necrotic area by TMF treatment

Extensive hepatocellular necrosis was observed in the control and TMF groups at 24 h after reperfusion (Fig. 3C). In contrast, no distinct areas of necrosis could be identified in the sham group. The necrotic area percentage in the TMF group was significantly lower than that in the control group (Fig. 3D).

### 3.5. Alleviation of apoptosis with TMF treatment

TUNEL-positive cells (round brown nuclei) were mainly observed in the control and TMF groups but rarely in the sham group (Fig. 4A). To quantify the expression of apoptosis-associated proteins, we measured Bcl-2, Bax, and cleaved caspase-3 in the liver tissues (Fig. 4B and Supplementary Fig. 1). The expression of BCL2 protein was significantly lower in the control and TMF groups than in the sham group ( $P < 0.001$ ), but there was no significant difference between the control and TMF groups ( $P = 0.979$ ). The expression of Bax protein in the control group was significantly higher than in the sham ( $P < 0.01$ ) and TMF ( $P < 0.05$ ) groups. The expression of C-cas3 protein in the control group was also significantly higher than in the sham ( $P < 0.01$ ) and TMF ( $P < 0.01$ ) groups.

### 3.6. Suppression of AhR expression by TMF administration

AhR expression was mainly observed in the control and TMF groups but rarely in the sham group (Fig. 5A). AhR proteins in the liver tissues were significantly higher in the control and TMF groups than in the sham group (Fig. 5B and Supplementary Fig. 2,  $P < 0.01$ ). The TMF group showed a significant decrease in AhR proteins than did the control group ( $P < 0.05$ ). In addition, as a result of analyzing the expression change of the AhR target genes, the expression of CYP1a1 in the control group was significantly higher than in the sham ( $P < 0.01$ ) and TMF ( $P < 0.01$ ) groups (Fig. 5C). The expression of CYP1b1 in the control group was also significantly higher than in the sham ( $P < 0.001$ ) and TMF ( $P < 0.001$ ) groups. The expression of AhRR was significantly higher in the control group than in

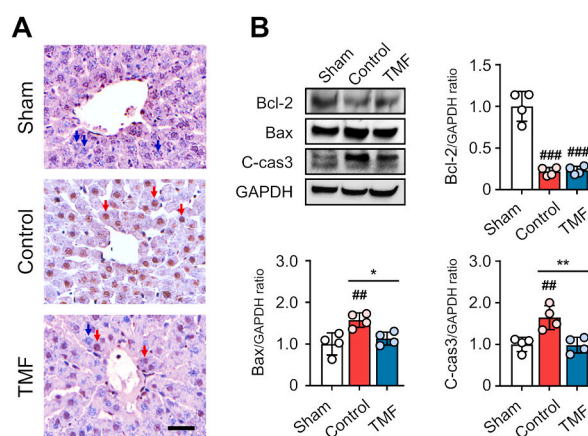


**Fig. 4. Reduction of apoptosis after 6,2',4'-trimethoxyflavone (TMF) administration** (A) Representative photomicrographs of terminal deoxynucleotidyl transferase-mediated dUTP nick-end labeling (TUNEL) staining 24 h after reperfusion (magnification  $\times 200$ , scale bar = 50  $\mu\text{m}$ ). Red arrows indicate apoptotic cells; blue arrows indicate viable cells. (B) The expression of BCL2 protein was significantly lower in the control and TMF groups than in the sham group. The expression of Bax protein in the control group was significantly higher than in the sham and TMF groups. The expression of C-cas3 protein in the control group was significantly higher than in the sham and TMF groups. Data are represented as means  $\pm$  standard deviations ( $n =$  four rats in each group).  $##P < 0.01$  vs. sham group;  $###P < 0.001$  vs. sham group;  $*P < 0.05$  vs. control group;  $**P < 0.01$  vs. control group. The full-length blots/gels are presented in Supplementary Fig. 1. (For interpretation of the references to color in this figure legend, the reader is referred to the Web version of this article.)

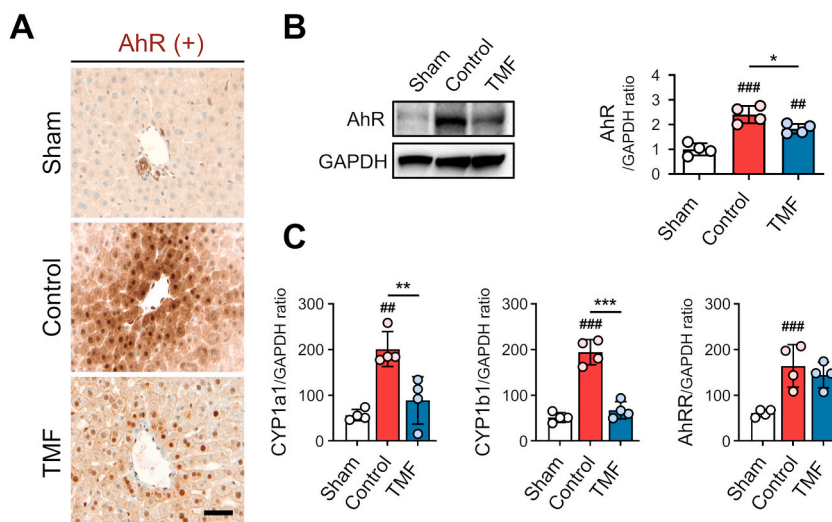


**Fig. 5.** Suppression of aryl hydrocarbon receptor (AhR) expression by 6,2',4'-trimethoxyflavone (TMF) treatment (A) Representative photomicrographs of AhR staining 24 h after reperfusion (magnification  $\times 200$ , scale bar = 50  $\mu$ m). (B) AhR proteins were significantly higher in the control and TMF groups than in the sham group. The TMF group showed a significant decrease in AhR proteins than did the control group. (C) The expression of CYP1a1 in the control group was significantly higher than in the sham and TMF groups. The expression of CYP1b1 in the control group was also significantly higher than in the sham and TMF groups. The expression of AhR was significantly higher in the control group than in the sham group. Data are represented as means  $\pm$  standard deviations ( $n = 4$  rats in each group). ## $P < 0.01$  vs. sham group; ### $P < 0.001$  vs. sham group; \* $P < 0.05$  vs. control group; \*\* $P < 0.01$  vs. control group; \*\*\* $P < 0.01$  vs. control group. The full-length blots/gels are presented in [Supplementary Fig. 2](#).

the sham group ( $P < 0.01$ ), but there was no significant difference between the control and TMF groups ( $P = 0.660$ ).

### 3.7. Changes in tryptophan metabolism due to hepatic I/R injury

The levels of TDO ( $P < 0.01$ ) and IDO1 ( $P < 0.001$ ) mRNA expression in the control group were significantly higher than in the sham group (Fig. 6A). Tryptophan levels were significantly lower in the control group than in the sham group ( $P < 0.01$ , Fig. 6B), and L-Kyn levels were significantly higher in the control group than in the sham group ( $P < 0.01$ ).

## 4. Discussion

In this study, we assessed the hepatoprotective effects of AhR antagonism on hepatic IR injury in rats. Rats treated with TMF at 10 min after ischemia had lower RE values and serum ALT and AST levels than did untreated rats at 3 h after reperfusion. After 24 h of reperfusion, TMF-treated rats had lower RE values,  $\Delta T1$  values, serum ALT levels, and necrotic area percentage than did untreated rats. In addition, the expression of the apoptosis-related proteins Bax and cleaved caspase-3 was lower in the TMF-treated rats than in the untreated rats. These results suggest that inhibiting AhR activation after ischemia ameliorates hepatic IR injury.

Under normal conditions, AhR remains inactive in the cytoplasm and is activated by endogenous ligands, such as L-Kyn [10], or exogenous ligands, such as 2,3,7,8-tetrachlorodibenzo-p-dioxin [20]. Recently, L-Kyn was found to accumulate in the brain during ischemia and induce the activation of AhR, exacerbating neuronal damage even after reperfusion [10]. Because a significant amount of L-Kyn is produced by tryptophan metabolism under TDO, brain-like phenomena due to ischemia are likely to occur in the liver as well [13]. However, to the best of our knowledge, there have yet to be studies on this. In this study, we investigated, for the first time, whether AhR antagonism after ischemia affects liver damage due to IR. Our results showed that AhR antagonism inhibited the progression of apoptosis and necrosis and that L-Kyn production was increased by tryptophan metabolism under TDO and IDO1. This suggests that L-Kyn accumulate owing to ischemia in the liver, as in the brain, and activate AhR, leading to hepatic IR injury.

The present study showed the inhibitory effect of apoptosis in animals administered with AhR antagonists after ischemia. However, it has not been elucidated which pathways downstream of AhR mediate hepatic IR injury. In the brain, several studies have reported that AhR inhibition reduces neuronal cell death and neurotoxicity [21,22]. In particular, cAMP response element binding protein (CREB) signaling has been reported as one of the downstream pathways caused by AhR activation [10]. The report suggests that AhR activation due to brain ischemia regresses CREB protein-dependent signaling and exacerbates brain damage. However, it is considered that AhR likely works with various sub-mechanisms. Therefore, further studies of sub-mechanisms, including alterations of CREB signaling induced by AhR activation in the liver, are needed.

Changes in serum ALT and AST levels in our study were used to evaluate changes in hepatic injury caused by IR. The serum ALT and AST levels are considered the representative markers of hepatocellular injury or necrosis [23,24]. Hepatocellular injury or necrosis causes ALT and AST leakage from hepatocytes into the blood; thus elevated serum ALT and AST levels suggest liver damage [25]. Our

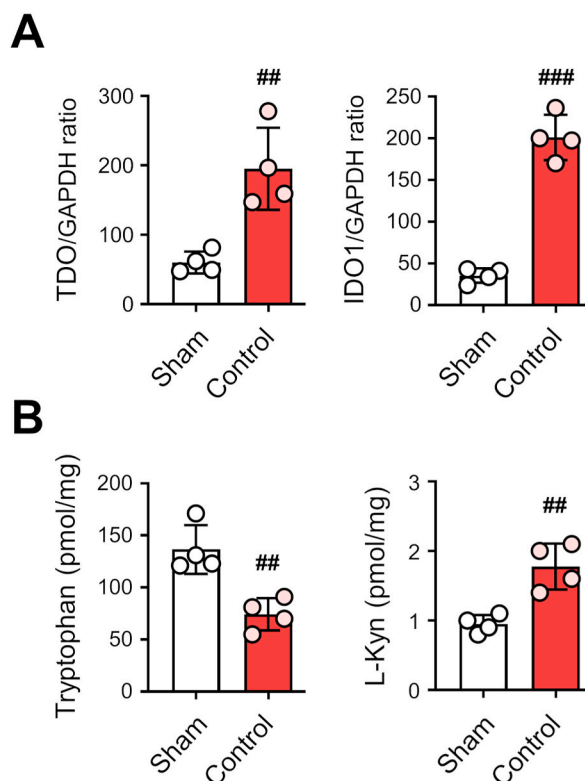


**Fig. 6.** Changes in tryptophan metabolism due to hepatic ischemia-reperfusion injury (A) The levels of tryptophan-2,3-dioxygenase (TDO) and indoleamine 2,3-dioxygenase 1 (IDO1) mRNA expression in the control group were significantly higher than in the sham group. (B) Tryptophan levels were significantly lower in the control group than in the sham group, and L-Kynurenine (L-Kyn) levels were significantly higher in the control group than in the sham group. Data are represented as means  $\pm$  standard deviations ( $n =$  four rats in each group). <sup>##</sup> $P < 0.01$  vs. sham group; <sup>###</sup> $P < 0.001$  vs. sham group.

study results indicate that TMF administration after ischemia contributes to the alleviation of IR-induced hepatocellular injury or necrosis. Furthermore, histological analysis also revealed a similar pattern of differences in the necrotic area. However, the mechanisms involved in the association between AhR activation and necrosis in this study have not been elucidated. Further research on this is needed.

We analyzed changes in liver function due to IR using Gd-EOB-DTPA, a paramagnetic hepatobiliary MR contrast agent. This was based on several reports that Gd-EOB-DTPA-enhanced MRI is suitable for evaluating liver function due to its organic anion transporting polypeptide-dependent hepatocyte-specific uptake and paramagnetic properties [26,27]. In particular, several reports have been demonstrated the effectiveness of liver function assessment using the SI-based indices of T1-WIs and the T1 relaxometry [16,18]. In this study, as a result of analyzing RE and LMR values reported to be highly correlated with liver function among SI-based indices [17], RE values were decreased in TMF-treated rats at 3 and 24 h after reperfusion compared to those of untreated rats. These results suggested that liver function was improved in the TMF-treated group. Based on T1 relaxometry, we analyzed T1<sub>post</sub> and  $\Delta$ T1 values [16,17]. At 24 h after reperfusion, the TMF-treated rats had decreased  $\Delta$ T1 values compared to those of untreated rats. These results indicated that liver function was improved in the TMF-treated rats.

There were two limitations in this study. First, we only tested a single dose of TMF in our analysis (5 mg/kg of TMF) that had been suggested previously by Cuartero et al. and Kwon et al. [10,12]. The concentration of TMF in the blood may be different depending on the concentration of TMF administered; thus, the effect on hepatic IR injury may also vary. Further studies are needed to find the optimal concentration to reduce hepatic IR injury. Second, we only observed that AhR expression at 24 h after reperfusion was significantly higher in the rats with hepatic IR injury than in the sham-operated and TMF-treated rats. This means that an increased expression of AhR may be one of the factors that play an important role in the progression of hepatic IR injury. However, in this study, the change in AhR expression was observed only 24 h after reperfusion, and it was not determined how the change in AhR expression changed or how long it lasted after reperfusion. Additional studies are needed to find the optimal timing of TMF administration by tracking changes in AhR expression after reperfusion.

Our findings demonstrated that post-ischemia administration of AhR antagonists has hepatoprotective effects that ameliorate hepatic IR injury. We propose that adequate AhR antagonist activity is a potential therapeutic approach for hepatic I/R injury. Nevertheless, further studies are needed to elucidate the mechanisms underlying the hepatoprotective effect to assess potential clinical applications of AhR antagonist administration.

## Author contribution statement

Jae-Im Kwon, Dong Cheol Woo, and Chul-Woong Woo conceived and designed the experiments, performed the experiments, analyzed and interpreted the data, and wrote the paper. Hwon Heo, Yeon Ji Chae, Joongkee Min, Do-Wan Lee, Sang Tae Kim, and Monica Young Choi performed the experiments and analyzed and interpreted the data. Yu Sub Sung, Kyung Won Kim, and Yoonseok Choi analyzed and interpreted the data and contributed reagents, materials, analysis tools, or data.

## Declaration of competing interest

The authors declare that they have no known competing financial interests or personal relationships that could have appeared to influence the work reported in this paper.

## Acknowledgments

We thank the Magnetic Resonance Core Facility at the ConveRgence mEDicine research cenTer (CREDIT), Asan Medical Center, for the MRI data acquisition and analysis. We would like to thank Editage ([www.editage.co.kr](http://www.editage.co.kr)) for English language editing. This study was supported by a grant (2019IL0602) from the Asan Institute for Life Sciences, Asan Medical Center, Seoul, Korea and the Basic Science Research Program through the National Research Foundation of Korea (NRF-2018R1C1B6003879).

## Appendix A Supplementary data

Supplementary data to this article can be found online at <https://doi.org/10.1016/j.heliyon.2023.e15596>.

## References

- [1] N. Kokudo, et al., The history of liver surgery: achievements over the past 50 years, *Ann. Gastroenterol. Surg.* 4 (2) (2020) 109–117.
- [2] L.A. Orci, et al., The role of hepatic ischemia-reperfusion injury and liver parenchymal quality on cancer recurrence, *Dig. Dis. Sci.* 59 (9) (2014) 2058–2068.
- [3] S. Yamazaki, T. Takayama, Current topics in liver surgery, *Ann. Gastroenterol. Surg.* 3 (2) (2019) 146–159.
- [4] V. Zabala, et al., Transcriptional changes during hepatic ischemia-reperfusion in the rat, *PLoS One* 14 (12) (2019) e0227038.
- [5] J. Bi, et al., Irisin alleviates liver ischemia-reperfusion injury by inhibiting excessive mitochondrial fission, promoting mitochondrial biogenesis and decreasing oxidative stress, *Redox Biol.* 20 (2019) 296–306.
- [6] L.Y. Guan, et al., Mechanisms of hepatic ischemia-reperfusion injury and protective effects of nitric oxide, *World J. Gastrointest. Surg.* 6 (7) (2014) 122–128.
- [7] C.A. Opitz, et al., An endogenous tumour-promoting ligand of the human aryl hydrocarbon receptor, *Nature* 478 (7368) (2011) 197–203.
- [8] M.S. Denison, S.R. Nagy, Activation of the aryl hydrocarbon receptor by structurally diverse exogenous and endogenous chemicals, *Annu. Rev. Pharmacol. Toxicol.* 43 (2003) 309–334.
- [9] O. Hankinson, The aryl hydrocarbon receptor complex, *Annu. Rev. Pharmacol. Toxicol.* 35 (1995) 307–340.
- [10] M.I. Cuartero, et al., L-kynurenine/aryl hydrocarbon receptor pathway mediates brain damage after experimental stroke, *Circulation* 130 (23) (2014) 2040–2051.
- [11] A. Padmanabhan, S.M. Haldar, Neuroprotection in ischemic stroke: AhR we making progress? *Circulation* 130 (23) (2014) 2002–2004.
- [12] J.I. Kwon, et al., Aryl hydrocarbon receptor antagonism before reperfusion attenuates cerebral ischaemia/reperfusion injury in rats, *Sci. Rep.* 10 (1) (2020), 14906.
- [13] A.R. Green, H.F. Woods, M.H. Joseph, Tryptophan metabolism in the isolated perfused liver of the rat: effects of tryptophan concentration, hydrocortisone and allopurinol on tryptophan pyrrolase activity and kynurenine formation, *Br. J. Pharmacol.* 57 (1) (1976) 103–114.
- [14] T. Karatzas, et al., Rodent models of hepatic ischemia-reperfusion injury: time and percentage-related pathophysiological mechanisms, *J. Surg. Res.* 191 (2) (2014) 399–412.
- [15] W.C. Chen, et al., Aryl hydrocarbon receptor modulates stroke-induced astrogliosis and neurogenesis in the adult mouse brain, *J. Neuroinflammation* 16 (1) (2019) 187.
- [16] C. Ma, et al., The hepatocyte phase of Gd-EOB-DTPA-enhanced MRI in the evaluation of hepatic fibrosis and early liver cirrhosis in a rat model: an experimental study, *Life Sci.* 108 (2) (2014) 104–108.
- [17] M. Nakagawa, et al., Measuring hepatic functional reserve using T1 mapping of Gd-EOB-DTPA enhanced 3T MR imaging: a preliminary study comparing with (99m)Tc GSA scintigraphy and signal intensity based parameters, *Eur. J. Radiol.* 92 (2017) 116–123.
- [18] M. Haimerl, et al., Gd-EOB-DTPA-enhanced MRI for evaluation of liver function: comparison between signal-intensity-based indices and T1 relaxometry, *Sci. Rep.* 7 (2017), 43347.
- [19] U.J. Bae, et al., SPA0355 attenuates ischemia/reperfusion-induced liver injury in mice, *Exp. Mol. Med.* 46 (2014) e109.
- [20] F.J. Quintana, et al., Control of T(reg) and T(H)17 cell differentiation by the aryl hydrocarbon receptor, *Nature* 453 (7191) (2008) 65–71.
- [21] M. Kajta, et al., Aryl hydrocarbon receptor-mediated apoptosis of neuronal cells: a possible interaction with estrogen receptor signaling, *Neuroscience* 158 (2) (2009) 811–822.
- [22] F.J. Sanchez-Martin, P.M. Fernandez-Salguero, J.M. Merino, Aryl hydrocarbon receptor-dependent induction of apoptosis by 2,3,7,8-tetrachlorodibenzo-p-dioxin in cerebellar granule cells from mouse, *J. Neurochem.* 118 (1) (2011) 153–162.
- [23] K.M. Jo, et al., Serum aminotransferase level in rhabdomyolysis according to concurrent liver disease, *Korean J. Gastroenterol.* 74 (4) (2019) 205–211.
- [24] P.T. Giboney, Mildly elevated liver transaminase levels in the asymptomatic patient (vol 71, pg 1105, 2005), *Am. Fam. Phys.* 72 (1) (2005) 41, 41.
- [25] T.H. Young, et al., Quantitative rat liver function test by galactose single point method, *Lab. Anim.* 42 (4) (2008) 495–504.
- [26] P.J. Meier, et al., Substrate specificity of sinusoidal bile acid and organic anion uptake systems in rat and human liver, *Hepatology* 26 (6) (1997) 1667–1677.
- [27] A. Nassif, et al., Visualization of hepatic uptake transporter function in healthy subjects by using gadoxetic acid-enhanced MR imaging, *Radiology* 264 (3) (2012) 741–750.